BBAA VI International Colloquium on:
Bluff Bodies Aerodynamics & Applications
Milano, Italy, July, 20-24 2008

AEROELASTICITY IDENTIFICATION OF SQUARE BUILDINGS WITH DIFFERENT HEIGHTS BY USING FORCED ACTUATION

Jong-Cheng Wu*, Yu-Yi Lin*, Cheng-Hsin Chang* and Ying-Chieh Chang*

*Professor (first author), Department of Civil Engineering, Tamkang University, Taipei, Taiwan
Tel: 886-2-26215656x2758, e-mail: joncheng@mail.tku.edu.tw

Keywords: Forced Actuation, High-rise Building, Aerodynamic Damping, Aerodynamic Stiffness, State Equation, Genetic Algorithm.

Abstract

This paper investigated the frequency-dependent aerodynamic damping and stiffness of high-rise buildings in the along-wind motion by utilizing forced actuation technique. A new approach that involves formulation in the form of state equations and employment of genetic algorithm for global minimization of the frequency response function curve-fitting was presented for identifying the frequency-dependent aerodynamic damping and stiffness. To demonstrate the approach presented, square-shape prisms with height/width ratios of 4, 7 and 10 (denoted as HB4, HB7 and HB10) to model three different high-rise buildings was used in the identification. The identified results show that their aerodynamic dampings are always negative and monotonically decreasing with the reduced velocity within the range of 60. Under the same reduced velocity, the absolute values of aerodynamic damping follow the trend of HB10>HB7>HB4. For the aerodynamic stiffness, as the reduced velocity increases, the aerodynamic stiffness for HB4 is monotonically increasing from zero while that for HB 10 is monotonically decreasing. However, the aerodynamic stiffness for HB7 is not significant.

1 INTRODUCTION

In the past decade, particularly in Asia area, the wind effect on high-rise buildings has become an inevitably important engineering issue. The newly completed Taipei 101 building (508 m) in Taipei is one of the typical examples. For such high-rise buildings, the different wind load generating mechanism that mutually interacts with the building response may be induced. The interaction between the structural response and wind load is generally called aero-elasticity. Many researches in earlier stage focused on the observation of this effect on a two-dimensional oscillating model (e.g., Nakamura and Mizota (1975), Bearman and Obasaju (1982)). In the last decade, few papers have investigated building aero-elasticity by using three-dimensional oscillating models, particularly for the across-wind motion (e.g., Sakamoto and Oiwake (1984), Vickery and Steckley (1993), and *etc*.).

Unlike the conventional approach, this paper focuses on the global effect of aero-elasticity existing in the along-wind motion of high-rise buildings by introducing the idea of frequency-dependent aerodynamic damping and stiffness. By utilizing forced actuation to the building, a new identification approach was developed. The approach involves formulation in the form

of state equations and employment of genetic algorithm (GA) for global minimization. To demonstrate the presented scheme, three square-shape prisms with the height/width ratios of 4, 7 and 10 to model three different types of high-rise buildings were placed in the wind tunnel of Department of Civil Engineering, Tamkang University, Taiwan for experimental identification.

2 FORMULATION

2.1 Equation of Motion of Wind-Excited Buildings Subjected to Forced Excitation

Consider a schematic diagram of the experimental setup shown in Fig. 1. The building model is a base-pivoted rigid model with a connecting rod rigidly jointed at the bottom. It is placed on the wind tunnel floor below which a shaking device is linked to the rod through a spring and dashpot. If the building model is simultaneously disturbed by the smooth wind flow and horizontal forced actuation from the shaking device, the equation of motion can be expressed as

$$J\,(\ddot{\theta} + 2\,\xi_\theta\,\omega_\theta\,\dot{\theta} + \omega_\theta^2\,\theta) = -c_\theta\,\dot{\theta}_0 - k_\theta\,\theta_0 + M(t) \quad (1)$$

in which J is the mass moment of inertia; $M(t)$ is the motion-induced moment; $\theta_0 = x_0/d$; $\omega_\theta = \sqrt{k_\theta/J}$; $k_\theta = kd^2$; $\xi_\theta = c_\theta/(2J\,\omega_\theta)$; $c_\theta = cd^2$.

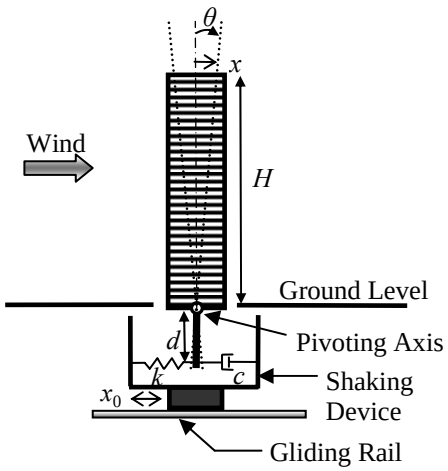

Fig.1: Schematic Diagram of Experimental Setup for Aeroelasticity Identification

2.2 Identification of Building Models

In absence of the wind flow disturbance (i.e., $M(t)$=0), the building response is entirely induced by the forced excitation from the shaking device. Thus, the frequency response function of θ induced by θ_0, $H^s_{\theta\theta_0}(i\omega)$, is $(-2\xi_\theta\omega_\theta\,(i\omega) - \omega_\theta^2)/((i\omega)^2 + 2\xi_\theta\omega_\theta(i\omega) + \omega_\theta^2)$. By curve-fitting the theoretical to experimental results for minimizing the weighted square error between each other, the coefficients $\xi_\theta\omega_\theta$ and ω_θ^2 can be determined. Besides, by incrementally attaching an additional mass to the system, the mass moment of inertia J can be identified by using the linear regression on $1/\hat{\omega}_\theta^2$ and ΔJ.

2.3 Identification of Aero-Elasticity in High-Rise Buildings

Under smooth wind flow and forced excitation, the aerodynamic moment is expressed as

$$M(t) = \rho U^2 D^2\,H\left\{K\,B_1^*(K)\,\frac{D\,\dot{\theta}(t)}{U} + K^2\,B_2^*(K)\,\theta(t)\right\} \quad (2)$$

in which D is characteristic width; $K = D\omega/U$ is the non-dimensional frequency; B_1^* and B_2^* are the dimensionless aerodynamic damping and stiffness. By taking Fourier transform on Eq. (2), the frequency response function of M induced by θ, $H_{M\theta}(iK)$, is expressed as

$$H_{M\theta}(iK) = \rho U^2 D^2\,H\,(i\,K^2\,B_1^* + K^2\,B_2^*) \quad (3)$$

Assuming that $H_{M\theta}(iK)$ can be further realized by an equivalent linear system, i.e.,

$$H_{M\theta}(iK) = \rho U^2 D^2 \, H\left[\frac{\bar{b}_n (iK)^n + \bar{b}_{n-1}(iK)^{n-1} + \cdots + \bar{b}_1 (iK) + \bar{b}_0}{(iK)^m + \bar{a}_{m-1}(iK)^{m-1} + \cdots + \bar{a}_1 (iK) + \bar{a}_0}\right] \; ; \; n = m+1 \qquad (4)$$

Or in the form of state equation in the time domain,

$$\dot{\mathbf{Z}} = \mathbf{A}_\theta \mathbf{Z} + \mathbf{B}_\theta \, \theta \; ; \; M = \mathbf{C}_\theta \mathbf{Z} + \sum_{j=0}^{2} Q_j \, \theta^j \qquad (5)$$

The substitution of Eq. (5) into Eq. (1) results in an overall state equation

$$\dot{\mathbf{q}} = \mathbf{A}\,\mathbf{q} + \mathbf{B}\left(-c_\theta \dot{\theta}_0 - k_\theta \, \theta_0\right) ; \; \theta = \mathbf{C}\,\mathbf{q} \qquad (6)$$

Therefore, the frequency response function θ induced by θ_0 is given by

$$H^W_{\theta\theta_0}(i\omega) = \left(\mathbf{C}\left((i\omega)\mathbf{I} - \mathbf{A}\right)^{-1}\mathbf{B}\right)\cdot\left(-c_\theta \, (i\omega) - k_\theta\right) \qquad (7)$$

By curve-fitting the theoretical to experimental results for minimizing the weighted square error between each other, the unknowns $\mathbf{A}_\theta$, $\mathbf{C}_\theta$, Q_0 and Q_1 can be determined. To achieve global minimum, genetic algorithm (GA) was used in searching the optimal solution. Once $\mathbf{A}_\theta$, $\mathbf{C}_\theta$, Q_0 and Q_1 are obtained, $H_{M\theta}(iK)$ in Eq. (4) can be computed, and thus B_1^* and B_2^* are related to its imaginary and real parts according to Eq. (3).

3 EXPERIMENTAL IDENTIFICATION

For basic comparison, the scaled building models used in the experiment are square-shape prisms with height/width ratios of 4, 7 and 10, denoted as HB4, HB7 and HB10, respectively. The values of ω_θ, ξ_θ and J identified are (6.51 Hz, 0.0076, 0.0233 kg-m^2), (3.52 Hz, 0.0075, 0.0793 kg-m^2), and (2.21 Hz, 0.0139, 0.1773 kg-m^2), respectively. For identifying the aero-elasticity, a band-limited white-noise of excitation from the shaking device was used to excite the building model while the smooth wind flow was simultaneously acting on the model. The experimental results of $H^W_{\theta\theta_0}(i\omega)$ under the wind flow at seven different mean wind velocities are plotted in Fig. 2 (a), (c), (e). As observed from Fig. 2, it is found that the along-wind flow suppresses the vibration and the suppression effect becomes stronger as the wind velocity increases. Following the GA minimization technique, each experimental curve of $H^W_{\theta\theta_0}(i\omega)$ was curve-fitted with n=3 and m=2 and the results are shown in Fig. 2 (b), (d), (f). Consequently, the values of B_1^* and B_2^* versus the non-dimensional wind velocity $\overline{U} = 2\pi / K$ are obtained.

4 CONCLUSIONS

This paper presents a new approach to identify the frequency-dependent aerodynamic damping and stiffness of high-rise buildings in the along-wind motion. The experimental setup in this approach was designed to focus on the global effect of aero-elasticity without considering the detail measurements for surface pressure as in the conventional way. By utilizing forced excitation technique, the approach involves formulation in the form of state equations and employment of genetic algorithm for global minimization. Three square-shape prisms with height/width ratios of 4, 7 and 10 to model three high-rise buildings were identified for comparison. The results show that the wind flow suppresses the along-wind vibration and the effect becomes stronger as the wind velocity increases. The aerodynamic damping B_1^* is always negative and monotonically decreasing with increasing $\overline{U}$ except for a small segment of HB10 at $\overline{U} > 60$. Under the same $\overline{U}$, the absolute values of aerodynamic

damping follow the trend of HB10>HB7>HB4. For the aerodynamic stiffness, as $\overline{U}$ increases, the value of B_2^* for HB4 is monotonically increasing from zero while that for HB10 is monotonically decreasing. The value of B_2^* for HB7 is monotonically decreasing from zero, however, its value does not have significant effect on the overall stiffness.

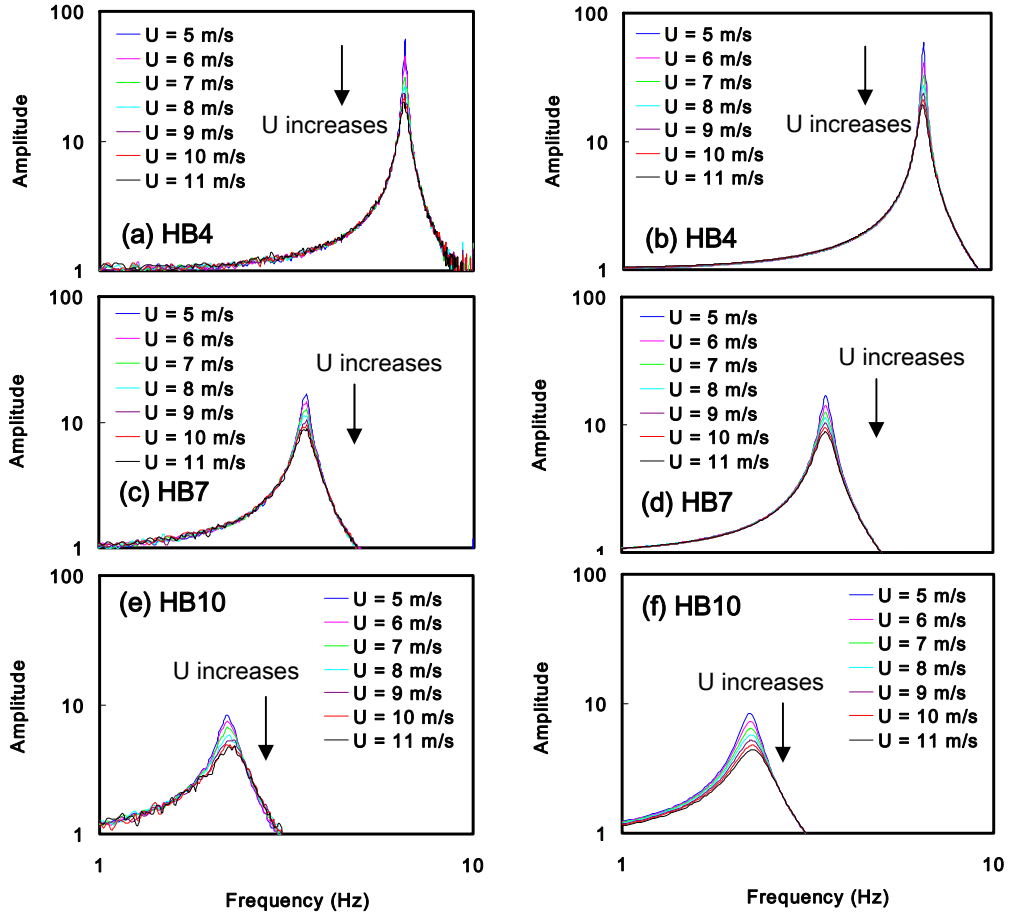

Fig 2: Frequency Response Functions of the Three Building Models under Different Wind Speeds: (a) Experimental Results of Model HB4; (b) Curve-Fitted Results of Model HB4; (c) Experimental Results of Model HB7; (d) Curve-Fitted Results of Model HB7; (e) Experimental Results of Model HB10; (f) Curve-Fitted Results of Model HB10.

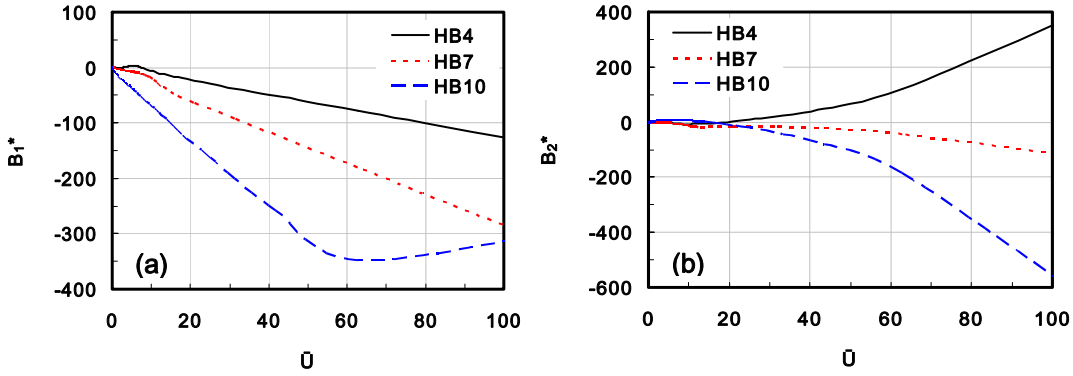

Fig 3: (a) Aerodynamic Damping B_1^*; (b) Aerodynamic Stiffness B_2^*